

# Automatic Data Augmentation by Learning the Deterministic Policy

Yinghuan Shi<sup>1</sup>, Tiexin Qin<sup>1</sup>, Yong Liu<sup>1</sup>, Jiwen Lu<sup>2</sup>, Yang Gao<sup>1</sup>, Dinggang Shen<sup>3</sup>

<sup>1</sup>Nanjing University, China <sup>2</sup>Tsinghua University, China <sup>3</sup>UNC Chapel Hill, USA

## Abstract

Aiming to produce sufficient and diverse training samples, data augmentation has been demonstrated for its effectiveness in training deep models. Regarding that the criterion of the best augmentation is challenging to define, we in this paper present a novel learning-based augmentation method termed as DeepAugNet, which formulates the final augmented data as a collection of several sequentially augmented subsets. Specifically, the current augmented subset is required to maximize the performance improvement compared with the last augmented subset by learning the deterministic augmentation policy using deep reinforcement learning. By introducing an unified optimization goal, DeepAugNet intends to combine the data augmentation and the deep model training in an end-to-end training manner which is realized by simultaneously training a hybrid architecture of dueling deep  $Q$ -learning algorithm and a surrogate deep model. We extensively evaluated our proposed DeepAugNet on various benchmark datasets including Fashion MNIST, CUB, CIFAR-100 and WebCaricature. Compared with the current state-of-the-arts, our method can achieve a significant improvement in small-scale datasets, and a comparable performance in large-scale datasets. Code will be available soon.

## 1. Introduction

Recent progress in deep learning has substantially improved the results of image classification or recognition tasks. With the goal of increasing the amount and diversity of the available training samples, data augmentation has shown its advantage for boosting the classification accuracy [16, 23]. By training the deep learning models on the original training images along with the obtained augmented images, a good generalization performance in the testing stage can be expected, especially for the small-scale datasets.

The most simple yet popular way of data augmentation is to perform the basic image preprocessing operators, *e.g.*, flipping, translation, rotation and color jittering, on the original images to generate the augmented images. This

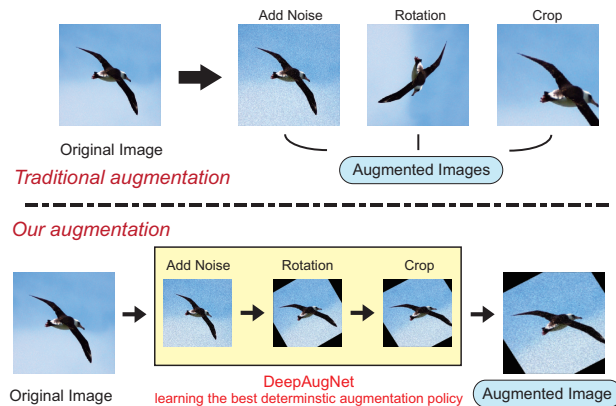


Figure 1. The major difference of traditional augmentation methods and our DeepAugNet. The traditional augmentation methods play a role as an individual image preprocessing step, while our method exploits the best sequential augmentation policy to maximize the performance improvement for the subsequent model training.

traditional setting could be regarded as an independent image preprocessing step before training the deep model, since the subsequent classification does not influence these pre-generated augmented images (*i.e.*, data augmentation does not get any feedback from the subsequent model training). Despite its success in some tasks, this kind of traditional augmentation still suffer from the major limitation of: **1) separation** – the data augmentation and model training are separated without a consistent objective, **2) redundancy** – the augmentation is usually random which might produce a large number of redundant samples, and **3) harmfulness** – some augmented images might be harmful for the model training.

Being aware of these limitations, the researchers are recently paying attention to the learning-based augmentation [1, 10, 7, 32, 3, 37]. According to our analysis, we notice that *the major bottleneck of the previous learning-based augmentation methods is that the criterion of the best augmentation is challenging to define*. Thus, these methods usually require the pre-defined assumption of data distribution before augmentation. For examples, the generative adversarial network (GAN) based augmentation methods assume the augmented and original images should belong to

a same data distribution [39, 14, 5]. The Mixup method [37] mainly focuses on the marginal region between different classes during augmentation. However, the augmentation results are largely influenced by these assumptions.

To relax these assumptions, we innovatively formulate the final augmented data as a collection of several sequentially augmented subsets, where the consecutive augmented two subsets should maximize the classification performance improvement. Thus, we present a novel method DeepAugNet, which directly optimizes the classification performance improvement in deep model training by automatically learning the best data augmentation policy in a deep reinforcement learning environment. Specifically, regarding that the original objective of augmentation is difficult to define and hard to optimize, we formulate it as a truncated objective where a trial-and-error strategy can be employed to combine the data augmentation and model training into a consistent goal. More precisely, the final augmented set in our method can be considered as a generalized union on several sequentially augmented subsets where each subset is required to maximize the performance improvement compared with the latest augmented subset on an additional surrogate model. To achieve this goal, we model our problem using a hybrid architecture of the dueling architectures-based deep Q-learning algorithm (Dueling DQN) which could be trained with the later surrogate model in an end-to-end manner. The major contributions of our method could be summarized into the following four folds:

- Our method is the first attempt to model automatic data augmentation as a deep reinforcement learning problem by learning a *deterministic* policy.
- The solution of final augmented set is formalized as to solve a generalized union on several sequentially augmented subsets that satisfy the maximum performance improvement.
- A joint scheme by integrating a hybrid architecture of Dueling DQN and a surrogate model is developed for effective policy learning.
- Extensive evaluation on various benchmark datasets including Fashion MNIST, CUB, CIFAR-100 and WebCaricature validates the advantage of our method.

## 2. Related Work

**Data Augmentation.** Basically, the common goal of different data augmentation methods is to generate the sufficient and various samples to augment the original training samples. According to previous studies, an appropriate data augmentation benefits the recognition performance compared with that of only using the original training samples. An initiatory yet frequently-used data augmentation

method is to directly perform some ordinary operators (*e.g.*, *flipping, rotation, translation*) on the original images to produce the augmented images [16, 23].

Recently, there have been a few attempts of learning-based augmentation and most of them use the GAN-based architecture which requires the augmented and original samples belong to a same distribution. Wang *et al.* [32] presented a meta learning-based GAN to produce additional training samples. Gurumurthy *et al.* [7] developed a model to adopt a mixture model to parameterize the latent generative space and meanwhile jointly learn the parameters of this mixture model and GANs. Gatys *et al.* [4] modeled the content and style loss separately which was helpful to generate new training images. Huang *et al.* [10] proposed a structure-aware image-to-image translation network and Antreas *et al.* [1] addressed the problem of predicting the label for the novel unseen classes according to the generated samples. Volpi *et al.* [30] also introduced a worst-case formulation over data distribution to tackle the augmentation on unseen domains. Recently, there are a very few attempts of nonGAN-based augmentation: Mixup [37] and AutoAugment [3]. In Mixup [37], a simple yet effective linear combination of in-between training samples was learned for augmentation. In AutoAugment [3], the random augmentation policy on dataset-level was exploited for effective augmentation.

**Deep Reinforcement Learning.** Deep reinforcement learning (DRL) wishes to learn a policy for an agent by a deep model in order to make a sequential decision for maximizing an accumulative reward [19, 20]. DRL has received considerable attention recently for its effectiveness of dealing with the high dimensional data in computer vision tasks. For example, Zhong *et al.* [38] presented a block-wise network generation pipeline to automatically establish the optimal network structure by sequentially choosing the component layers. Tang *et al.* [28] introduced a method of selecting the most beneficial frames from video to boost the performance of action recognition. Song *et al.* [26] employed DRL method to generate a sequence of artificial user input for interactive image segmentation. Also, Han *et al.* [8] adjusted the location of context box and object box to maximize the segmentation performance. Park *et al.* [21] modeled the optimal global enhancement in a DRL manner. For object localization and tracking, Caicedo *et al.* [2] trained an agent learning algorithm to deform a bounding box with some simple transformation actions in order to correctly localize a target object. Ren *et al.* [22] and Guo *et al.* [6] introduced the DRL-based methods for object tracking. Kong *et al.* [15] proposed a collaborative algorithm with multi-agents to localize different objects. Although DRL methods are playing a more important role in various vision tasks, to exploit the automatic data augmentation using DRL is still in its early stage.

**Remark.** Despite the success of previous learning-based augmentation methods in various tasks, most of them

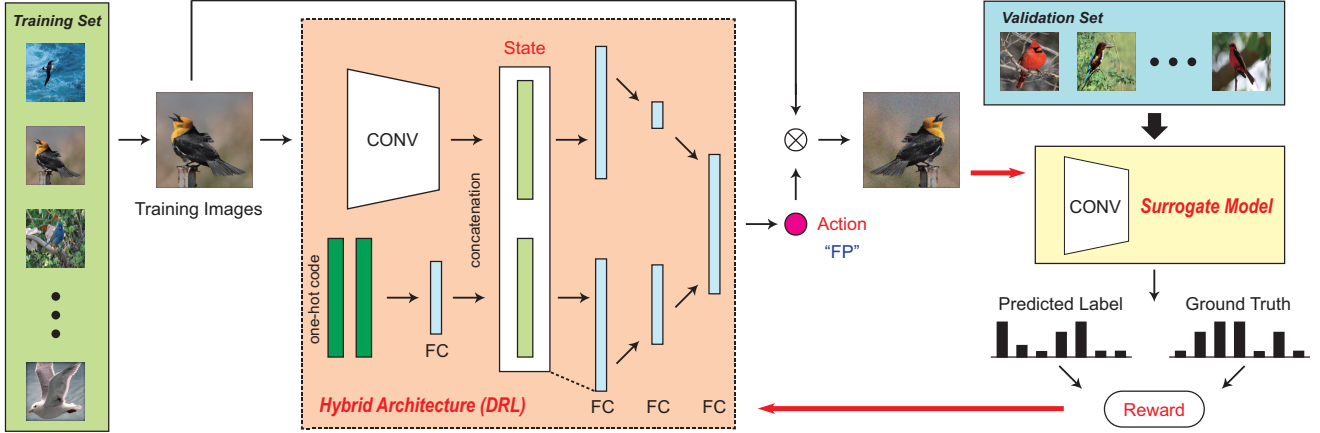


Figure 2. The framework of our method DeepAugNet.

[1, 10, 7, 32, 37] require a predefined assumption for the data distribution before augmentation (e.g., training and testing samples belonging to a same distribution, the augmented samples distributed in marginal region between different classes, etc.). Compared with them, our method directly optimizes the performance improvement without any assumptions on the original distribution.

In addition, although AutoAugment [3] also employs DRL to learn the policies, our method is largely different from AutoAugment: **1)** our method is sample-wise (i.e., learning the best policy for the samples in a batch) while AutoAugment is dataset-wise (i.e., learning the uniform action for the entire dataset), **2)** our method learns the deterministic policy while AutoAugment learns the random policy, where the deterministic policy could guide more robust results, and **3)** our method introduces the terminal action while AutoAugment only learns the combination of two actions.

### 3. Our Method: DeepAugNet

#### 3.1. Problem Formulation

**Analysis.** Our DeepAugNet intends to learn a best way of data augmentation to benefit the subsequent deep learning models. Basically, jointly training the data augmentation and classification models in an end-to-end manner is extremely difficult to realize due to the following key challenges: **1)** the searching space of the data augmentation on the available training images is very huge which might bring into a severe overfitting problem. **2)** The best augmentation is hard to quantify as a traditional supervised learning problem. In particular, given the training set  $\mathbf{X}$ , we wish to jointly learn an augmented set  $\mathbf{X}'$  and a prediction function (i.e., deep model)  $f$  parameterized by  $\theta$  to minimize the following objective as follows:

$$\min_{\theta, \mathbf{X}'} \sum_{x_i \in \mathbf{X} \cup \mathbf{X}'} L(f(x_i; \theta_{\mathbf{X} \cup \mathbf{X}'}), y_i), \quad (1)$$

where  $x_i$  and  $y_i$  ( $1 \leq i \leq |\mathbf{X} \cup \mathbf{X}'|$ ) are the  $i$ -th training sample and its ground truth label, respectively.  $L(\cdot)$  is a loss function (i.e., we adopt the popularly-used cross entropy function) to measure the difference between the prediction  $f(x_i; \theta_{\mathbf{X} \cup \mathbf{X}'})$  and ground truth  $y_i$ .  $\theta_B$  indicates that the model parameter  $\theta$  is trained on the set  $B$ . However, we notice that Eqn. (1) is difficult to solve since **1)** the augmentation set  $\mathbf{X}'$  is hard to represent, **2)**  $\mathbf{X}'$  and  $\theta$  are interacted which is difficult to optimize, and **3)** the overfitting issue might happen in training because  $\mathbf{X}'$  is actually generated from  $\mathbf{X}$  without introducing any additional data.

Therefore, to overcome these limitation, we present a truncated two-layer objective of Eqn. (1) as below:

$$\begin{aligned} \min_{\theta} \quad & \sum_{x_i \in \mathbf{X} \cup g^*(\mathbf{X})} L(f(x_i; \theta_{\mathbf{X} \cup g^*(\mathbf{X})}), y_i) \\ \text{s.t.} \quad & g^* = \arg \min_g \sum_{x_j \in \mathbf{X}^*} L(f(x_j; \theta_{\mathbf{X} \cup g(\mathbf{X})}), y_j), \end{aligned} \quad (2)$$

where  $\mathbf{X}^*$  is an additional validation set (i.e.,  $\mathbf{X}^* \cap \mathbf{X} = \emptyset$ ) playing a supervision role which does not involve into the training process to avoid overfitting.  $\mathbf{X}^*$  can be either sampled from the training set  $\mathbf{X}$  or an existing validation set<sup>1</sup>.  $g(\cdot)$  indicates that we wish to learn a transformation to generate the augmented data from the observed training data. The way of introducing  $g(\cdot)$  is more feasible than that of directly learning the augmentation data from a random initialization or a Gaussian noise. In this meaning, the input of  $g(\mathbf{X})$  is the original training set and the output is the augmentation set.

Considering the fact that  $g(\mathbf{X})$  is non-trivial to define, we innovatively model the estimation of  $g(\mathbf{X})$  as a generalized union of different subsets as follows:

$$g(\mathbf{X}) = \bigcup_{i=1}^N g^T(x_i), \quad (3)$$

<sup>1</sup>In practice, we split the dataset into training, validation and testing set. The validation set is firstly used to adjust the hype-parameters, and then acts as the environment in reinforcement learning to return the reward.

where  $T$  is the maximum number of steps (*i.e.*, terminal step) and  $N$  is the cardinality of original training set (*i.e.*,  $N = |\mathbf{X}|$ ).  $g^T(x_i)$  is the generated augmentation subset at the terminal step. To establish the connection between the different subsets, we approximate this estimation of  $g(\mathbf{X})$  as an MDP (Markov decision process) task [27] in a deep reinforcement learning framework. Specifically, we first define several basic actions (*e.g.*, *rotation*, *flip* and *crop*) and then obtain the sequential combination of these defined actions for  $t$ -th step subset as follows:

$$g^t(\mathbf{X}) = \begin{cases} g^{t-1}(\mathbf{X}) \otimes a^t, & t \geq 1 \\ \mathbf{X}, & t = 0, \end{cases} \quad (4)$$

where  $g^{t-1}(\mathbf{X}) \otimes a^t$  indicates that the images in  $g^{t-1}(\mathbf{X})$  perform the  $t$ -th step action  $a^t$  to form the generated images. Finally, a series of sets  $g^1(\mathbf{X}), g^2(\mathbf{X}), \dots, g^T(\mathbf{X})$  are obtained with their generalized union as the final data augmentation set.

As analyzed, our DeepAugNet actually contains two major stages: the action learning stage and the surrogate training stage. We visually illustrate the pipeline of our proposed DeepAugNet in Fig. 2.

**Action Learning.** By receiving the delayed reward and current input set, the action learning stage tries to learn a best action by maximizing the curriculum reward. Typically, we train a state extraction network to learn the current state according to the inputs. To avoid the possible overfitting caused by repeating performing a same action during the training procedure, we punish this action-repeating strategy by a typical penalty for better generalization. To achieve this, we proposed a hybrid architecture for Dueling DQN [33] by introducing the one-hot code of latest two actions as an additional parameter. The output of this one-hot code is combined with the output of the state extraction network by three layer fully connected network to output the learned action. Finally, this action is used to generate the new images as a guidance.

**Surrogate Training.** In the surrogate training stage, we introduce the surrogate model trained on the separate validation set which does not involve in the training to reduce the computational burden and prevent the overfitting. Typically, the input of the surrogate training stage is the  $t$ -th step augmented sample and the output is the calculated reward. To compute the effective reward, we intend to maximize the performance improvement between two consecutive steps. Specifically, two consecutive subsets (*i.e.*,  $g^t(\mathbf{X})$  and  $g^{(t+1)}(\mathbf{X})$ ) should show a maximized improvement on the reward. At  $t$ -th step, we train this surrogate model by fine-tuning the model  $f$  with the current generated augmentation subset  $g^t(\mathbf{X})$ . This process continues until the convergence of the reward, which indicates the data augmentation will not improve the performance anymore.

## 3.2. Network Components

**State.** Given a current image  $x_i$  as input, the state  $s^t$  can be defined as the output of the state extraction network  $\phi$  as follows.

$$s^t = \phi(x_i). \quad (5)$$

Note that, we adopt different state extraction networks  $\phi$  according to the property of different datasets. For example, for small-scale images with size smaller than  $50 \times 50$  (*e.g.*, Fashion MNIST), we directly use the raw images as the state since its corresponding state space is relatively not too huge thus an agent with only a few layers is able to learn. While for large-size images, aiming to prevent from the huge state space, we employ the pre-trained convnet (*e.g.*, VGG) as the state extraction network with the corresponding output (*i.e.*, feature vector) as the state.

**Action.** During the training procedure, each agent outputs an action  $a^t$  according to the current state  $s^t$ . We formally introduce ten types of basic actions, which contains: **FP** (*flip the image*), **RT** (*rotate the image*), **AN** (*add noise*), **WP** (*warp the image*), **CL** (*crop from left side*), **CR** (*crop from right side*), **CT** (*crop from top side*), **CB** (*crop from bottom side*), **ZM** (*zoom in the image into 1.1x*) and **TM** (*terminate the processing*). Specifically, for **RT**, we perform the rotation on the current image by  $30^\circ$  clockwise. For **AN**, the Gaussian noise is added to the normalized image to form a new image. For **WP**, the current image is distorted by the PiecewiseAffine operator in `imgaug` library<sup>2</sup>. For four different crop action (*i.e.*, **CL**, **CR**, **CT** and **CB**), the respective 10-20% boundary regions will be cropped from the current image according to different datasets.

**Reward.** The reward directly influences the final classification performance. In each step, the agent is required to choose an action  $a^t$  by receiving a reward  $r^t$ . With the goal of learning the best data augmentation policy, we maximize the improvement on the validation set  $\mathbf{X}^*$  by measuring the difference between the prediction  $f(x_j; \theta)$  and the ground truth  $y_j$  using the loss function  $L(\cdot)$ . Specifically, the  $t$ -th step reward  $r^t$  is formally written as follows:

$$r^t = \begin{cases} J^{t-1} - J^t, & a^t \neq \mathbf{TM} \\ 10(J^{t-1} - J^t), & a^t = \mathbf{TM}, \end{cases} \quad (6)$$

where  $J^t$  indicates the the  $t$ -th step loss in the surrogate model:

$$J^t = \sum_{x_j \in \mathbf{X}^*} L(f(x_j; \theta_{\mathbf{X} \cup \{x_i^t\}}), y_j), \quad (7)$$

where  $x_i^t$  denotes the result of the  $t$ -th step on the  $i$ -th training sample as  $x_i^t = g^t(x_i^{t-1})$ . In Eqn. (7),  $f(x_j; \theta_{\mathbf{X} \cup \{x_i^t\}})$  indicates the network trained by fine-tuning  $f(x_j; \theta_{\mathbf{X}})$  with  $x_i^t$ .

<sup>2</sup><https://imgaug.readthedocs.io/en/latest/>

### 3.3. Training

To efficiently train our DeepAugNet, we propose to extend the Dueling DQN [33] with a hybrid loss to prevent the overfitting for training our augmentation policy. The Dueling DQN was proven to be powerful in estimating the Q-function by integrating two functions: the state value function (parameterized by  $\beta$ ) and the state-dependent action advantage function (parameterized by  $\sigma$ ). Specifically, during the training procedure, we wish to learn the current estimation of Q-function  $Q(s^t, a^t; \gamma, \omega, \beta, \sigma)$  to guide the next action selection for an agent, where  $\gamma$  and  $\omega$  are the parameters of the state extraction network and one-hot code, respectively. Formally, Q-learning iteratively adopts the Bellman equation to update the selection policy in a recursive manner as follow:

$$Q(s^t, a^t; \gamma, \omega, \beta, \sigma) = r^t + \rho \max_{a^{t+1}} Q(s^{t+1}, a^{t+1}; \gamma, \omega, \beta, \sigma), \quad (8)$$

where  $\rho$  is the discount factor. Also, inspired by Dueling DQN, we defined the hybrid Q-function as follows:

$$Q(s^t, a^t; \gamma, \omega, \beta, \sigma) = V(s^t; \gamma, \omega, \sigma) + A(s^t, a^t; \gamma, \omega, \beta) - \frac{1}{|A|} \sum_{a^{t+1}} A(s^t, a^{t+1}; \gamma, \omega, \beta),$$

where  $V(s^t; \gamma, \omega, \sigma)$  and  $A(s^t, a^t; \gamma, \omega, \beta)$  are the state-value and advantage function [33], respectively. More details could be referred to [33]. We summarize the training procedure in Algorithm 1.

**Implementation.** We implement our model on a GPU server with NVIDIA GTX 1080Ti using PyTorch platform. the SGD (stochastic gradient descent) algorithm is used for optimization. Also, we use Imgaug library for efficient implementation of basic actions.  $\rho$  is set to 1 in this paper for Eqn. (8). For the learning rate, we adopt the different settings for different datasets which will be detailed in the experiment part. We establish individual respective experience relay for each action to prevent from the severe imbalance action selection which might cause overfitting.

**Acceleration.** Since a separate validation set is introduced to compute the reward in our method, the computational time is influenced by the scale of this validation set. To accelerate the training time, a feasible way is to selectively reduce the number of samples in validation set. In our implementation, we propose to sample the more difficult images with higher probability to form a reduced validation set from a large scale training set where the difficulty is defined according to the classification confidence on a pre-trained model.

## 4. Experiments

We present the qualitative and quantitative results of the proposed DeepAugNet, and compare it with state-of-the-art methods developed for image recognition task. For

---

### Algorithm 1: DeepAugNet

---

**Data:** Training set  $\mathbf{X}$ , validation set  $\mathbf{X}^*$   
**Result:** Augmentation set  $\mathbf{X}'$

```

1 for epoch = 1, ..., n do
2   Initialize  $\mathbf{X}' = \emptyset$ ;
3   for  $i = 1, \dots, |\mathbf{X}|$  do
4      $t \leftarrow 1$ ;
5     repeat
6        $s^t \leftarrow$  Compute the state by Eqn. (5);
7        $a^t \leftarrow$  Compute the action by Eqn. (8);
8        $x'_i \leftarrow$  Performing action  $a^t$  on  $x_i$ ;
9        $\theta \leftarrow$  Optimize the model parameter by
        fine-tuning with  $x'_i$ ;
10       $r^t \leftarrow$  Compute the reward by Eqn. (7);
11       $x_i \leftarrow x'_i$ ;
12       $t \leftarrow t + 1$ ;
13    until  $a^t = \text{TM}$  or  $t = T$ ;
14     $\mathbf{X}' = \mathbf{X}' \cup \{x_i\}$ ;
15    Compute the TD error as [33];
16  end
17 end

```

---

full investigation, we evaluate our method on four different datasets, including Fashion MNIST, CUB (Caltech-UCSD Birds), WebCaricature and CIFAR-100. The selected datasets vary from different sizes, resolution and classes as illustrated in Table 1.

Note that, for fair comparison, all the listed baselines used the same base network for surrogate model training. Also, the hyper parameters in the respective models of all these methods are kept to be same.

Table 1. The details of different datasets.

Datasets	# Samples	# Class	Resolution
CUB-20	1,153	20	224 × 224 × 3
WebCaricature	1,414	20	224 × 224 × 3
Fashion MNIST	60,000	10	28 × 28
CIFAR-100	60,000	100	32 × 32 × 3

### 4.1. Results on CUB-20

**Setting.** To investigate the performance of our method on the small-sized but large-resolution dataset, we extract a sub-set from the CUB dataset [34] with 20 classes including 1153 images. We split the training, validation and testing data with the ratio 0.5, 0.2 and 0.3. Each image is with RGB channels of size 224 × 224 × 3. We use the pre-trained VGG [25] as the state extraction network to produce a 4,096-dimensional state vector for each image. The base network for surrogate model is also VGG with kernel size of 12. The learning rates in 1-150, 150-250 and 250+ epoches are set to 0.1, 0.01 and 0.001, respectively. When training the VGG, we set the number of epoches to 300 and the batch size to 32. Also, the learning rate in fine-tuning is set to

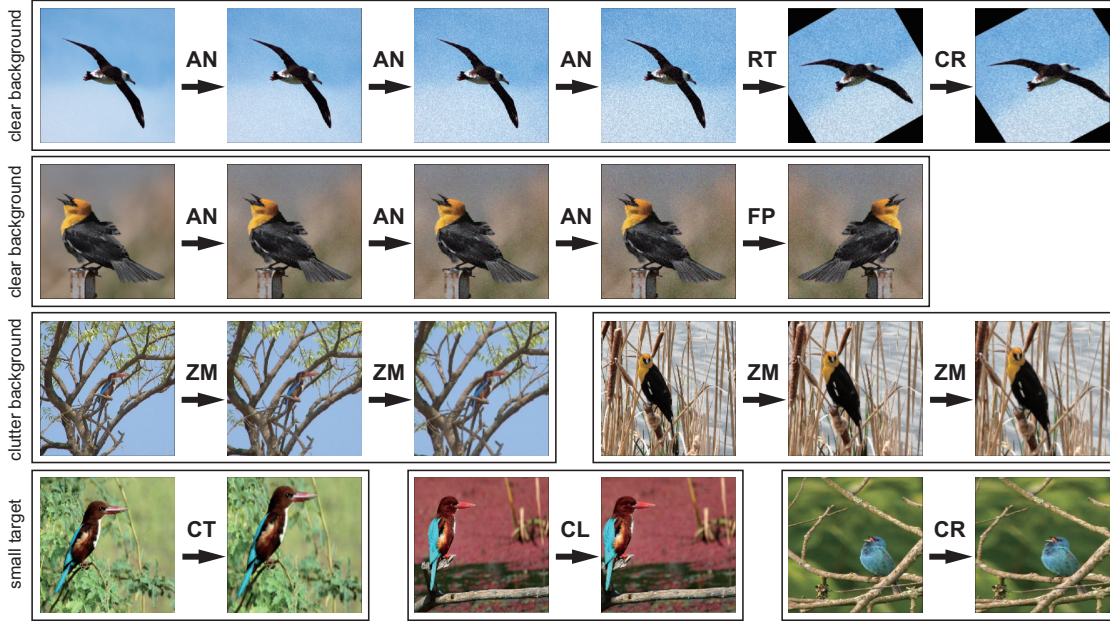


Figure 3. The visual examples of automatic data augmentation steps on CUB-20. **AN** (*adding noise*) is usually selected to add the difficulty for the images with clear background which are easy to classify. **ZM** (*zoom in*) is frequently selected for the images with relative clutter background since the foreground birds are hard to be observed. Also, crop operators are useful to increase the size of foreground birds for small-size targets.

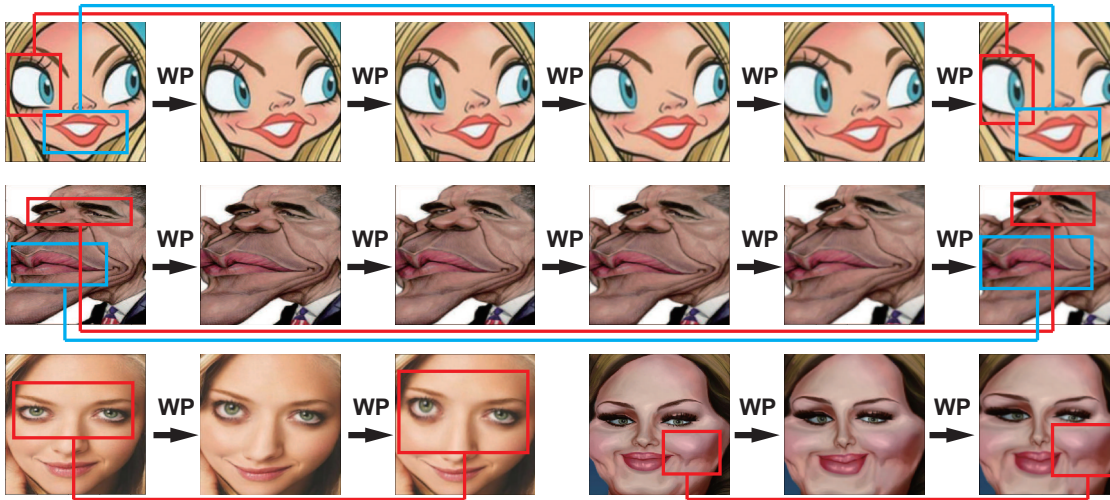


Figure 4. The visual examples of automatic data augmentation steps on WebCaricature. **WP** (*warp*) is the most frequently used action. We could notice that the specific properties are enhanced, *e.g.*, eyes and mouths with the bounding boxes of a same color between the original image and final augmented image.

0.001. The exploration rate for Dueling DQN decays from 1 and stops at 0.01. The size of each experience buffer is set as 10,000 transitions.

We introduce the VGG without any data augmentation (termed **VGG-WA**) and the VGG with traditional augmentation (termed **VGG-TA**) as the two preliminary baselines since our DeepAugNet is also trained on the same VGG. The traditional augmentation in VGG-TA includes the operators as *flipping*, *rotation* and *warp* *etc.* We maintain the same number of augmentation samples for both VGG-TA and DeepAugNet. Directly comparing these three methods

(*i.e.*, VGG-WA, VGG-TA and DeepAugNet-VGG) is helpful to reveal the role of data augmentation in the recognition task. Besides, for comparison with the current state-of-the-arts, we introduced the three recent published learning-based augmentation methods, *i.e.*, **Mixup** [37], **AutoAugment** [37] and **Neural + No Loss** [31]. For the AutoAugment and Mixup, we directly used their released implementation. For Neural + No Loss, we re-implement it by ourselves.

**Results.** We present the test accuracy of these baselines in Table 2. Our result is better than the methods with-

out augmentation, with traditional augmentation, and with learning-based augmentation. Moreover, we illustrate several visual examples of our automatic augmentation steps on CUB-20 in Fig. 3. From Fig. 3, we observe that: (1) **AN** (*adding noise*) is usually selected to add the difficulty for the images with clear background which are easy to classify, (2) **ZM** (*zoom in*) is frequently chosen for the images with relative clutter background since the foreground birds are hard to be observed and (3) crop operators are useful to increase the size of foreground birds for small-size targets<sup>3</sup>.

Table 2. Test accuracy of different baselines on CUB-20.

Method	Accuracy (%)	Venue
VGG-WA [25]	81.88	–
VGG-TA [25]	81.99	–
Mixup [37]	80.09	ICLR 2018
AutoAugment [3]	76.61	Arxiv 2018
Neural + No Loss [31]	80.24	CVPR 2018
<b>DeepAugNet-VGG</b>	<b>86.31</b>	Proposed

Table 3. Test accuracy of different baselines on WebCaricature.

Method	Accuracy (%)	Venue
VGG Face-WA	79.33	–
VGG Face-TA	82.50	–
Mixup [37]	89.39	ICLR 2018
Neural + No Loss [31]	85.05	CVPR 2018
<b>DeepAugNet-VGG Face</b>	<b>96.64</b>	Proposed

## 4.2. Results on Caricature Recognition

**Setting.** The WebCaricature [11, 12] is a photograph-caricature dataset with the large intra-personal variations of caricatures. We employ the same ratios for training, validation and testing as that in CUB-20. The number of classes is 20 and the total number of images is 1,414. To eliminate the factors that are not relevant to the recognition in caricatures, we generate a bounding box to capture human face according to the facial landmarks. We adopt the pre-trained VGG-Face [25] as the state extraction network. For the architecture of surrogate model, we delete the last linear layer of VGG-Face and meanwhile add two new fully connected layers of (2622, 1024) and (1024, 20). During training, we load the pre-trained VGG-Face parameters and fine-tune the network globally, which is demonstrated to be more promising. The learning rate of our model is initialized as 0.1 with a decay of  $0.98^{\text{epoch}}$ , and the total number of epoches is set to 150. The parameters in deep reinforcement learning are maintained to be same as that in CUB-20. We did not include AutoAugment here since it does not contain the warp operator which is quite useful in this task.

**Results.** We report the test accuracy of these baselines in Table 3. Our result outperforms these baselines with a large margin. According to our observation in Fig. 4, **WP** (*warp*) is the most frequently used action. We could notice that the

<sup>3</sup><https://github.com/WonderSeven/DeepAugNet/blob/master/demo.mp4>

specific properties are enhanced, *e.g.*, eyes and mouths with the bounding boxes of a same color between the original image and final augmented image.

## 4.3. Results on Fashion MNIST

**Setting.** Fashion MNIST dataset<sup>4</sup> consists of 40,000 training, 10,000 validation and 10,000 testing samples. There are in total 10 classes: T-shirt, trouser, pullover, dress, coat, sandal, shirt, sneaker, bag and ankle boot. Regarding the images in Fashion MNIST are relatively small sized, we directly use the raw images as the states for training our DeepAugNet. In our implementation, we use the learning rate decay: the learning rates in 1-150, 150-250 and 250+ epoches are set to 0.1, 0.01 and 0.001, respectively. For the base network of surrogate model, we adopt the AlexNet [16] which is good enough to obtain promising results in Fashion MNIST. Typically, we introduce the AlexNet without any data augmentation (termed **AlexNet-WA**) and the AlexNet with traditional augmentation (termed **AlexNet-TA**) as the two preliminary baselines since our DeepAugNet is also trained on the same AlexNet. The traditional augmentation in AlexNet-TA includes the operators as *flipping*, *rotation* and *warp* *etc.* Besides, we also introduce **SqueezeNet** [13] and **Yu *et al.*'s method** [36] to investigate the current level on the shallow networks (*i.e.*, less than 10 layers). We did not include AutoAugment since most of its actions are specifically designed for color images.

Table 4. Test accuracy of different baselines on Fashion MNIST.

Method	Accuracy (%)	Venue
SqueezeNet-200 [13]	90.00	Arxiv 2016
Yu <i>et al.</i> [36]	~ 88.70	ECCV 2018
AlexNet-WA [16]	91.29	–
AlexNet-TA [16]	90.51	–
Mixup [37]	<b>92.10</b>	ICLR 2018
Neural + No Loss [31]	91.19	CVPR 2018
<b>DeepAugNet-AlexNet</b>	<b>91.54</b>	Proposed

Table 5. Transfer experiment on Fashion MNIST.

Source	Target	Accuracy (%)	
		DeepAugNet-AlexNet	AlexNet-TA
500	1,000	80.86	80.09
500	5,000	85.69	85.40
500	10,000	87.43	86.62
500	50,000	90.91	90.51
1,000	5,000	85.90	85.40
1,000	10,000	87.35	86.62
1,000	50,000	90.78	90.51
5,000	10,000	86.94	86.62
5,000	50,000	90.63	90.51
10,000	50,000	91.25	90.51

**Results.** The test accuracy of these baselines is reported in Table 4. Our result outperforms all the baselines except

<sup>4</sup><https://www.kaggle.com/zalando-research/fashionmnist>

the Mixup. We illustrate several visual examples of our automatic augmentation steps on Fashion MNIST in Fig. 5, where the actions **RT** (*rotation*) and **FP** (*flip*) are the most frequently selected to produce the sufficient samples with different orientations.

To exploit the efficacy of policy learned in different sizes of set, we investigated the policy transfer in Fashion MNIST, showing the learned policies are actually helpful to improve the recognition results in Table 5. Specifically, taking the first line of Table 5 as an example, we first train an agent on the training set only including 500 samples. Then, we directly use the learned policy to augment the training set with another 1,000 samples. The testing accuracy for this strategy is 80.86 % which outperforms the baseline (traditional augmentation) trained on 1,000 samples with accuracy of 80.09 %. The results demonstrate the policies learned by our method on a smaller size set (**Source**) work well on another bigger set (**Target**).

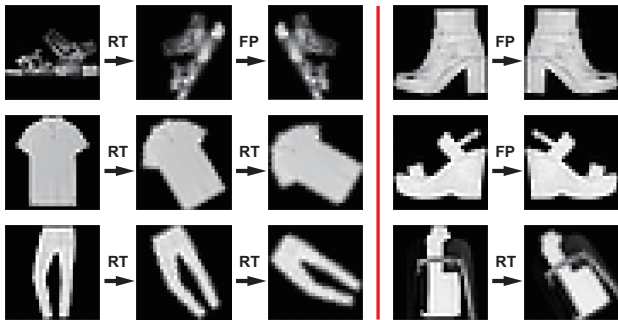


Figure 5. The visual examples of automatic data augmentation steps on Fashion MNIST. The actions **RT** (*rotation*) and **FP** (*flip*) are the most frequently used to generate the skew presentation for upright objects.

#### 4.4. Results on CIFAR-100

**Setting.** CIFAR-100 dataset<sup>5</sup> consists of 50,000 training and 10,000 testing samples with in total 100 classes. To accelerate the training procedure, we randomly sample 4,000 images as the reduced training set and 1,000 images as the validation set from training set. There does not exist any overlap between these two sets. Besides, we use a small network (*i.e.*, DenseNet-BC [9] with 50 layers<sup>6</sup>) as our surrogate model to get the augmentation policy. For dealing with large-scale dataset, we increase the batch size during learning the policy.

Like Fashion MNIST, we directly use the raw images as the states for training our DeepAugNet. In our implementation, we use the cosine annealing learning rate decay [18]. For the final classification model, we adopt the DenseNet-BC with 100 layers. Typically, we introduce the DenseNet-BC without any data augmentation (termed

<sup>5</sup><https://www.cs.toronto.edu/~kriz/cifar.html>

<sup>6</sup><https://github.com/bamos/densenet.pytorch>

**DenseNet-WA**) and the DenseNet-BC with traditional augmentation (termed **DenseNet-TA**) as the two preliminary baselines. Also, two learning-based methods: Mixup and AutoAugment are introduced as the additional baselines.

Table 6. Test accuracy of different baselines on CIFAR-100.

Method	Accuracy (%)	Venue
DenseNet-WA [9]	73.42	CVPR 2017
DenseNet-TA [9]	74.41	CVPR 2017
Mixup [37]	<b>75.28</b>	ICLR 2018
AutoAugment [3]	74.96	Arxiv 2018
<b>DeepAugNet-DenseNet</b>	75.11	Proposed

**Results.** The test accuracy of these baselines is reported in Table 6. Our result ranks the 2<sup>nd</sup> place in all the listed baselines. Also, we show several visual examples of our automatic augmentation steps on CIFAR-100 in Fig. 6. Intuitively, the actions **ZM** (*zoom in*), **WP** (*warp*) and **AN** (*adding noise*) are the most frequently used.

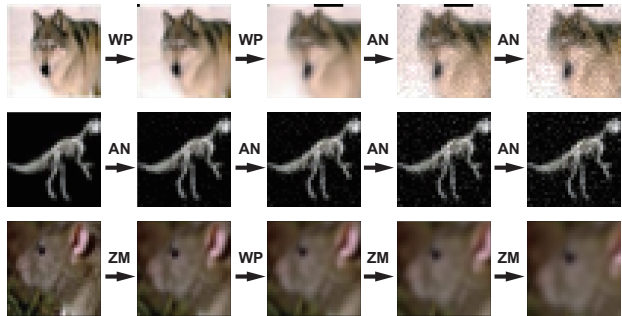


Figure 6. The visual examples of automatic data augmentation steps on CIFAR-100.

**Discussion.** Compared with the current state-of-the-arts learning-based augmentation methods, we can infer that our method can achieve a significant improvement in small-scale datasets, and a comparable performance in large-scale datasets. This is because that, when the limited samples in small-scale datasets are not sufficient to train a promising model, the predefined assumption of data distribution might not guarantee an effective augmentation. Also, thanks to the deterministic policy, our method can obtain the robust results in both small- and large-scale datasets.

## 5. Conclusion

Regarding that the criterion of best augmentation is difficult to define, we innovatively attempt to model the automatic augmentation as a deep reinforcement learning problem by learning a deterministic augmentation policy. To achieve this goal, a joint learning scheme by integrating a hybrid architecture of Dueling DQN and a surrogate model is developed where the learning policy guides the augmentation by directly optimizing the performance improvement. Extensive experiments validated the effectiveness of our

DeepAugNet. Our future directions include the extension to other vision tasks (e.g., segmentation) and the combination to other DRL architectures [24, 17, 29, 35]. Also, we will exploit the different action selection preferences in different datasets to guide better action design and initialization.

## References

- [1] A. Antoniou, A. Storkey, and H. Edwards. Data augmentation generative adversarial networks. *arXiv:1711.04340*, 2018. 1, 2, 3
- [2] J. C. Caicedo and S. Lazebnik. Practical block-wise neural network architecture generation. In *ICCV*, 2015. 2
- [3] E. D. Cubuk, B. Zoph, D. Mane, V. Vasudevan, and Q. V. Le. Autoaugment: Learning augmentation policies from data. *arxiv.org/abs/1805.09501*, 2018. 1, 2, 3, 7, 8
- [4] L. A. Gatys, A. S. Ecker, and M. Bethge. Image style transfer using convolutional neural networks. In *CVPR*, 2016. 2
- [5] I. J. Goodfellow, J. Pouget-Abadie, M. Mirza, B. Xu, D. Warde-Farley, S. Ozair, A. Courville, and Y. Bengio. Generative adversarial networks. In *NIPS*, 2014. 2
- [6] M. Guo, J. Lu, and J. Zhou. Dual-agent deep reinforcement learning for deformable face tracking. In *ECCV*, 2018. 2
- [7] S. Gurumurthy, R. K. Sarvadevabhatla, and R. V. Babu. Deligan : Generative adversarial networks for diverse and limited data. In *CVPR*, 2017. 1, 2, 3
- [8] J. Han, L. Yang, D. Zhang, X. Chang, and X. Liang. Reinforcement cutting-agent learning for video object segmentation. In *CVPR*, 2018. 2
- [9] G. Huang, Z. Liu, L. van der Maaten, and K. Q. Weinberger. Densely connected convolutional networks. In *CVPR*, 2017. 8
- [10] S.-W. Huang, C.-T. Lin, S.-P. Chen, Y.-Y. Wu, P.-H. Hsu, and S.-H. Lai. Auggan: Cross domain adaptation with gan-based data augmentation. In *ECCV*, 2018. 1, 2, 3
- [11] J. Huo, Y. Gao, Y. Shi, and H. Yin. Variation robust cross-modal metric learning for caricature recognition. In *ACM Multimedia Thematic Workshops*, 2017. 7
- [12] J. Huo, W. Li, Y. Shi, Y. Gao, and H. Yin. Webcaricature:a benchmark for caricature recognition. In *BMVC*, 2018. 7
- [13] F. N. Iandola, S. Han, M. W. Moskewicz, K. Ashraf, W. J. Dally, and K. Keutzer. Squeezenet: Alexnet-level accuracy with 50x fewer parameters and <0.5mb model size. *arXiv:1602.07360*, 2016. 7
- [14] P. Isola, J.-Y. Zhu, T. Zhou, and A. A. Efros. Image-to-image translation with conditional adversarial networks. In *Computer Vision and Pattern Recognition (CVPR), 2017 IEEE Conference on*, 2017. 2
- [15] X. Kong, B. Xin, Y. Wang, and G. Hua. Collaborative deep reinforcement learning for joint object search. In *CVPR*, 2017. 2
- [16] A. Krizhevsky and I. S. and Geoffrey E. Hintonl. Imagenet classification with deep convolutional neural networks. *NIPS*, 2012. 1, 2, 7
- [17] T. P. Lillicrap, J. J. Hunt, A. Pritzel, N. Heess, T. Erez, Y. Tassa, D. Silver, and D. Wierstra. Continuous control with deep reinforcement learning. *arxiv.org/abs/1509.02971*, 2016. 9
- [18] I. Loshchilov and F. Hutter. Sgdr: Stochastic gradient descent with warm restarts. In *ICLR*, 2017. 8
- [19] V. Mnih, K. Kavukcuoglu, D. Silver, and et al. Playing atari with deep reinforcement learning. *NIPS Deep Learning workshop*, 2013. 2
- [20] V. Mnih, K. Kavukcuoglu, D. Silver, and et al. Human-level control through deep reinforcement learning. *Nature*, 2015. 2
- [21] J. Park, J.-Y. Lee, D. Yoo, and I. S. Kweon. Distort-and-recover: Color enhancement using deep reinforcement learning. In *CVPR*, 2018. 2
- [22] L. Ren, X. Yuan, J. Lu, M. Yang, and J. Zhou. Deep reinforcement learning with iterative shift for visual tracking. In *CVPR*, 2017. 2
- [23] O. Ronneberger, P. Fischer, and T. Brox. U-net: Convolutional networks for biomedical image segmentation. In *MICCAI*, 2015. 1, 2
- [24] J. Schulman, F. Wolski, P. Dhariwal, A. Radford, and O. Klimov. Proximal policy optimization algorithms. *arxiv.org/abs/1707.06347*, 2017. 9
- [25] K. Simonyan and A. Zisserman. Very deep convolutional networks for large-scale image recognition. *arXiv:1409.1556*, 2014. 5, 7
- [26] G. Song, H. Myeong, and K. M. Lee. Seednet: Automatic seed generation with deep reinforcement learning for robust interactive segmentation. In *CVPR*, 2018. 2
- [27] R. S. Sutton and A. G. Barto. Introduction to reinforcement learning. In *1st ed. Cambridge, MA, USA: MIT Press*, 1998. 4
- [28] Y. Tang, Y. Tian, J. Lu, P. Li, and J. Zhou. Deep progressive reinforcement learning for skeleton-based action recognition. In *CVPR*, 2018. 2
- [29] A. S. Vezhnevets, S. Osindero, T. Schaul, N. Heess, M. Jaderberg, D. Silver, and K. Kavukcuoglu. Feudal networks for hierarchical reinforcement learning. *arxiv.org/abs/1703.01161*, 2017. 9
- [30] R. Volpi, H. Namkoong, O. Sener, J. Duchi, V. Murino, and S. Savarese. Generalizing to unseen domains via adversarial data augmentation. In *NIPS*, 2018. 2
- [31] J. Wang and L. Perez. The effectiveness of data augmentation in image classification using deep learning. In *CVPR*, 2018. 6, 7
- [32] Y.-X. Wang, R. Girshick, M. Herbert, and B. Hariharan. Low-shot learning from imaginary data. In *CVPR*, 2018. 1, 2, 3
- [33] Z. Wang, T. Schaul, M. Hessel, H. van Hasselt, M. Lanctot, and N. de Freitas. Dueling network architectures for deep reinforcement learning. In *ICML*, 2016. 4, 5
- [34] P. Welinder, S. Branson, T. Mita, C. Wah, F. Schroff, S. Belongie, and P. Perona. Caltech-ucsd birds 200. In *CNS-TR*, 2010. 5
- [35] M. Wulfmeier, P. Ondruska, and I. Posner. Maximum entropy deep inverse reinforcement learning. *arxiv.org/abs/1507.04888*, 2015. 9
- [36] B. Yu, T. Liu, M. Gong, C. Ding, and D. Tao. Correcting the triplet selection bias for triplet loss. In *ECCV*, 2018. 7
- [37] H. Zhang, M. Cisse, Y. N. Dauphin, and D. Lopez-Paz. Mixup: Beyond empirical risk minimization. In *ICLR*, 2018. 1, 2, 3, 6, 7, 8

- [38] Z. Zhong, J. Yan, W. Wu, J. Shao, and C.-L. Liu. Practical block-wise neural network architecture generation. In *CVPR*, 2018. 2
- [39] Zhu, Jun-Yan, T. Park, P. Isola, and A. A. Efros. Unpaired image-to-image translation using cycle-consistent adversarial networks. In *Computer Vision (ICCV), 2017 IEEE International Conference on*, 2017. 2